Validation of Crush Energy Calculation Methods for Use in Accident Reconstructions by Finite Element Analysis

Author(s): Shusuke Numata, Koji Mizuno, Daisuke Ito, Dai Okumura and Hisashi Kinoshita

Source: *SAE International Journal of Transportation Safety*, Vol. 6, No. 2 (2018), pp. 133-146

Published by: SAE International

Stable URL: https://www.jstor.org/stable/10.2307/26562393

REFERENCES
Linked references are available on JSTOR for this article:
https://www.jstor.org/stable/10.2307/26562393?seq=1&cid=pdf-reference#references_tab_contents
You may need to log in to JSTOR to access the linked references.

JSTOR is a not-for-profit service that helps scholars, researchers, and students discover, use, and build upon a wide range of content in a trusted digital archive. We use information technology and tools to increase productivity and facilitate new forms of scholarship. For more information about JSTOR, please contact support@jstor.org.

Your use of the JSTOR archive indicates your acceptance of the Terms & Conditions of Use, available at https://about.jstor.org/terms

SAE International is collaborating with JSTOR to digitize, preserve and extend access to *SAE International Journal of Transportation Safety*

This content downloaded from
66.194.72.152 on Thu, 01 Jul 2021 17:05:51 UTC
All use subject to https://about.jstor.org/terms

ARTICLE INFO
Article ID: 09-06-02-0009
Copyright © 2018
SAE International
doi:10.4271/09-06-02-0009

Validation of Crush Energy Calculation Methods for Use in Accident Reconstructions by Finite Element Analysis

Shusuke Numata, Koji Mizuno, Daisuke Ito, and Dai Okumura, *Nagoya University, Japan*
Hisashi Kinoshita, *DENSO Corporation, Japan*

Abstract

The crush energy is a key parameter to determine the delta-V in accident reconstructions. Since an accurate car crush profile can be obtained from 3D scanners, this research aims at validating the methods currently used in calculating crush energy from a crush profile. For this validation, a finite element (FE) car model was analyzed using various types of impact conditions to investigate the theory of energy-based accident reconstruction.

Two methods exist to calculate the crush energy: the work based on the barrier force and the work based on force calculated by the vehicle acceleration times the vehicle mass. We show that the crush energy calculated from the barrier force was substantially larger than the internal energy calculated from the FE model. Whereas the crush energy calculated from the vehicle acceleration was comparable to the internal energy of the FE model.

In full frontal impact simulations, the energy of approach factor (EAF) has a linear relation with the residual crush, which had been validated in previous experimental studies. In our study using FE analysis, we found that the slope of EAF versus the residual crush was comparable with that of the dynamic crush energy versus the dynamic crush for crashes at 55 km/h. Using this slope and the residual crush from a 55 km/h impact test, the slope and the intercept of the EAF vs. residual crush can be determined using only one crash test. A database of the slopes and the intercepts was made using Japan New Car Assessment Program (JNCAP) tests. In offset impact simulations, the crush energy calculated from the crush profile agreed with the internal energy of the car FE model when at least one front rail was involved. In oblique impacts, the correction factor for crush energy is not necessary within 20 degrees of principal direction of force of the car's longitudinal axis.

History

Received: 16 Nov 2017
Revised: 30 Jul 2018
Accepted: 01 Aug 2018
e-Available: 04 Oct 2018

Keywords

Crush energy, Delta-V, Accident reconstruction, Finite element analysis

Citation

Numata, S., Mizuno, K., Ito, D., Okumura, D. et al., "Validation of Crush Energy Calculation Methods for Use in Accident Reconstructions by Finite Element Analysis," *SAE Int. J. Trans. Safety* 6(2):133–145, 2018, doi:10.4271/09-06-02-0009.

ISSN: 2327-5626
e-ISSN: 2327-5634

This content downloaded from
66.194.7[illegible] on Thu, 01 Jul 2021 17:05:53 UTC
All use subject to https://about.jstor.org/terms

Introduction

In undertaking accident reconstructions, the vehicle crush energy is one of the key parameters to determine the delta-V and the barrier equivalent velocity. The theory to calculate the crush energy had been established by the 1990s. From crash tests, Emori [1] found that the vehicle velocity has a linear relation with residual crush in full frontal tests. Based on this relation and the assumption that the structure shows homogeneous behavior along the vehicle width, Campbell [2] expressed the crush energy using the impact force per crush width and developed a calculation method of crush energy for various vehicle crush profiles. This method was included in the damage analysis algorithm of the CRASH program to calculate the delta-V from crush energy [3]. Expanding from Campbell's work, Prasad [4] proposed the Energy of Approach Factor (EAF), which has a linear relation with vehicle crush C as follows:

$$\sqrt{\frac{2E_A}{w}} = d_0 + d_1 C \qquad \text{Eq. (1)}$$

where E_A is the total energy dissipated during the approach period (crush energy) and w is the vehicle width. The intercept d_0 and the slope d_1 are called the crush stiffness coefficients and can be calculated for various vehicles in full frontal tests conducted for the new car assessment program (NCAP) [4]. In order to determine d_0 and d_1, at least two crash tests with different vehicle impact velocities are necessary. Usually full frontal tests in NCAP are used for the high-velocity tests. When low-velocity tests are not available, the intersection d_0 is determined such that no residual crush occurs at some threshold. A typical threshold is 5 mph (8 km/h) [5]. The theory of calculating the crush energy from crush profile in various force-crush models is reviewed in Reference [6].

Kerkhoff et al. [7] and Varat et al. [8] examined EAF using crashes ranging from low to high impact velocities. They proposed a bilinear approximation for EAF vs. crush. The slope of EAF changed around the impact velocity of 30 mph because the passenger compartments at that time collapsed at higher impact velocities. However, the passenger compartments of today's current cars do not collapse at such high velocities. This trend was observed after the offset impact tests had been introduced into the regulatory and NCAP tests. Therefore, it is necessary to reexamine the EAF at higher impact velocities.

Assuming the uniform stiffness of the vehicle along crush width, the maximum crush energy (E_A) of the vehicle can be calculated for various shapes of crush profiles [2, 3]. E_A is calculated as:

$$E_A = K_1 d_0^2 + K_2 d_0 d_1 + K_3 d_1^2 \qquad \text{Eq. (2)}$$

$$\begin{aligned} K_1 &= \frac{w}{2} \\ K_2 &= \frac{w}{10}\left\{C_1 + 2\left(C_2 + C_3 + C_4 + C_5\right) + C_6\right\} \\ K_3 &= \frac{w}{30}\left\{C_1^2 + 2\left(C_2^2 + C_3^2 + C_4^2 + C_5^2\right) + C_6^2 \right. \\ &\quad \left. + C_1C_2 + C_2C_3 + C_3C_4 + C_4C_5 + C_5C_6\right\} \end{aligned} \qquad \text{Eq. (3)}$$

FIGURE 1 Force and crush component in oblique impact.

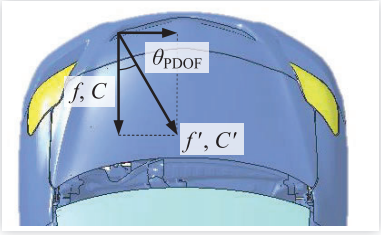

© SAE International

where C_i (i = 1, …, 6) is the residual crush depth across the crush width w. The assumption of homogeneous stiffness of cars was verified in experimental studies [2]. However, it was not investigated systematically whether this assumption is true for various overlap ratios in impacts.

The direction of impulse, referred to as principal direction of force (PDOF), can be defined at an angle θ_{PDOF} from the vehicle longitudinal direction (Figure 1).

© 2018 SAE International. All Rights Reserved.

This content downloaded from 66.194.72.152 on Thu, 01 Jul 2021 17:05:51 UTC
All use subject to https://about.jstor.org/terms

Case 2:19-cv-01338-JCC Document 80-1 Filed 07/14/21 Page 4 of 15

The maximum crush energy E'_A is calculated with force f' and the crush C' in the impact direction:

$$E'_A = \int f' dC' \quad \text{Eq. (4)}$$

The force vector and crush vector can be resolved into the vehicle lateral and longitudinal directions, and the force and crush magnitude of the vehicle longitudinal direction are $f = f' \cos \theta_{PDOF}$ and $C = C' \cos \theta_{PDOF}$. The crush energy can be calculated by using E_A using crush depth measured along the car longitudinal direction by:

$$E'_A = E_A \left(1 + \tan^2 \theta_{PDOF}\right) \quad \text{Eq. (5)}$$

where the term $(1 + \tan^2 \theta_{PDOF})$ is a correction factor. Although it is not necessary to input the PDOF in the calculation of delta-V in planar impact mechanics on the basis of momentum conservation [9], it should be required in the crush energy basis accident reconstruction. In oblique impacts, the energy is calculated using crush depths measured in the vehicle longitudinal direction, and it is corrected using Equation 5. Equation 5 is based on the assumption that the vehicle structure shows isotropic behavior in oblique impacts [10].

The vehicle stiffness and the vehicle crush energy are determined based on crush force-displacement curves. In general, the product of vehicle mass and the acceleration at the passenger compartment is used for calculating the crush force. Instead of vehicle acceleration, the barrier force in full frontal impact tests is also used to express directly the impact force at the crash interface. In some research studies [11, 12], the barrier force-displacement characteristics are approximated with nonlinear equations. Oga et al. [13] used the barrier force data of the high-resolution load cells with 125 mm × 125 mm size from JNCAP. The energy distribution cell diagrams in vehicle longitudinal and lateral directions were presented for various vehicle types. According to these diagrams, vehicles absorb the crush energy at the locations where the front rails and the engine impact.

At present, 3D laser measurement is applied to measure the vehicle crush after a collision. Using the 3D measurement, it is expected that the crush energy can be calculated with higher accuracy. The residual crush that is used to calculate the crush energy can be measured accurately from the cross section (2D *xy*-plane) cut at the height of the front rails from the 3D crush profile. Thus, it will be useful to reexamine the theory of crush energy currently used in accident reconstruction. Previous research studies have established a theory of crush energy calculation from crush profile based on crash tests. In this research, a finite element (FE) model of a small car was used to investigate the currently used theory of vehicle crush energy calculation, which was introduced by Campbell [2] and modified by Prasad [4]. In using FE analysis, impact conditions can be changed easily, and parameters which are difficult to obtain in tests can be readily examined. Moreover, the internal energy of the FE model is available from the output of the calculations, and can be compared to that calculated using the crush profile based on the theory currently used in accident reconstruction (Equations 1-4). Event data recorders (EDRs), which have been installed in many cars since the end of the 1990s, can be used to determine the delta-V. However, the delta-Vs determined from the EDRs contain some errors [14]. Thus it would be useful to compare the delta-Vs determined from the EDRs with those based on the crush energy because they are based on different principles.

FIGURE 2 The car FE model.

© SAE International

Method

An FE model of a small car (2010 Toyota Yaris model) developed by the National Crash Analysis Center was used for the analyses (Figure 2). This model (left-hand drive) was validated in full frontal and offset impact tests by its developers [15]. The general purpose nonlinear dynamic analysis code LS-DYNA version R7.1.1 was used for the analyses.

© 2018 SAE International. All Rights Reserved.

This content downloaded from
66.194.72.152 on Thu, 01 Jul 2021 17:05:51 UTC
All use subject to https://about.jstor.org/terms

FIGURE 3 The residual crush measured for the FE model.

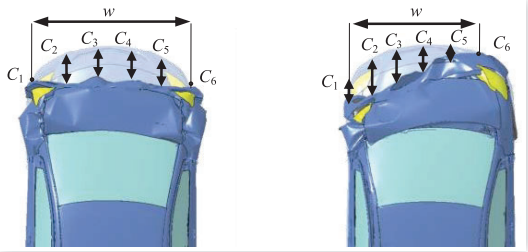

© SAE International

In FE analysis, the acceleration, velocity, and deformation of selected nodes are obtained. Moreover, the kinetic energy, internal energy, sliding interface (contact) energy, and hourglass energy can be obtained for each structure. The internal energy is energy absorbed by the materials of the various vehicle components as a result of their deformation, and is calculated using the stress and strain. In this research, the hourglass energy was included in the internal energy calculation. Hence, the energy loss is the sum of the internal energy and the sliding energy in the FE simulation calculations. The crush energy used in accident reconstruction can be expressed from the subtraction of kinetic energy from the total energy (energy loss). Hence, the sum of internal energy and sliding energy in FE model is equivalent to the crush energy. Using the sum of internal energy and sliding energy obtained from the output in FE analysis as a reference value, this was compared to the crush energy which was calculated from the crush profile using Equation 2 for various crash configurations. In full frontal impact, the sliding energy is so small that the internal energy was used as a reference value.

For the FE model, the residual crush was measured from the initial car shape in the car's longitudinal direction (C_1 to C_6) at the frame height (Figure 3). At the outside locations of the front rails, the residual crush at the wheel axis height was measured because the wheel is a structure that can transmit the crash forces. In the full frontal impact, the crush width w that the vehicle had contact with the barrier was used at the low velocity due to the rounded front shape of the car, whereas the crush width becomes the same as the vehicle total width at a high velocity. The average residual crush C_{Ave} was calculated as:

$$C_{Ave} = \frac{1}{5}\left(\frac{C_1}{2} + C_2 + C_3 + C_4 + C_5 + \frac{C_6}{2}\right) \quad \text{Eq. (6)}$$

Model Validation

In this research, full frontal impact tests of a Toyota Belta (the sedan model equivalent to the Toyota Yaris except that it has a right-hand steering wheel) were conducted at 55 km/h and 80 km/h were used to validate the model. The correlation analysis (CORA) rating method [16] was used to evaluate the level of correlation between accelerations of the passenger compartment in the FE simulation and that in the impact tests. The CORA combines a corridor rating and cross-correlation rating. The CORA rating ranges from 0 (no correlation) to 1 (perfect match). The residual crush of the right and the left front rails was compared between the FE model and the test results, and the errors of the residual crush of the FE model relative to that of the tests were calculated.

Crush Force

FIGURE 4 One-dimensional spring-mass system of vehicle with engine in impact against the rigid wall.

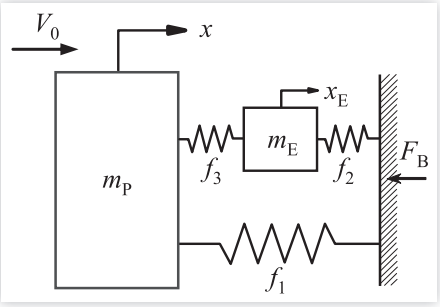

© SAE International

The crush energy is the work done by the vehicle crush force. Two ways to express the crush forces were examined: one was the product of the vehicle mass and the passenger compartment acceleration, and the other was the barrier force as measured using the load cell mounted on the barrier face. Consider the spring-mass model shown in Figure 4. This model includes the engine to consider the engine dump (i.e., the engagement of the engine with the barrier) against the barrier during impact since the engine impact on the wall has a substantial influence on the barrier force in full frontal rigid barrier tests [17, 18]. In designating the mass and the displacement of the passenger compartment as m_P and x, that of the engine as m_E and x_E, the vehicle mass m (i.e., $m_P + m_E$), the impact velocity as V_0, and the force acting on the spring $f_i(d)$ as a function of its deformation d, the equations of motion of the system after the engine impact the barrier are as follows:

$$m_P\ddot{x} = -f_1(x) - f_3(x - x_E) \quad \text{Eq. (7)}$$

© 2018 SAE International. All Rights Reserved.

This content downloaded from 66.194.72.152 on Thu, 01 Jul 2021 17:05:51 UTC
All use subject to https://about.jstor.org/terms

Case 2:19-cv-01338-JCC Document 80-1 Filed 07/14/21 Page 6 of 15

$$m_E \ddot{x}_E = -f_2(x_E) + f_3(x - x_E) \quad \text{Eq. (8)}$$

Note that the springs can be nonlinear and that the reaction force $f_i(d)$ can be expressed as a function of d. The effect of the gap between the engine and the barrier is also included in f_2 (e.g., $f_2(x_E) = 0$ while x_E is less than the gap between the engine and the barrier). The barrier force F_B is expressed by the sum of the inertia forces as:

$$F_B = f_1(x) + f_2(x_E) = -m_P \ddot{x} - m_E \ddot{x}_E \quad \text{Eq. (9)}$$

The deformation energy is calculated by summing the work done by all the springs in the system U_S and is expressed as follows:

$$\begin{aligned} U_S &= \int f_1(x)dx + \int f_2(x_E)dx_E + \int f_3(x - x_E)d(x - x_E) \\ &= \int \{f_1(x) + f_3(x - x_E)\}dx + \int \{f_2(x_E) - f_3(x - x_E)\}dx_E \\ &= -\int m_P \ddot{x}dx - \int m_E \ddot{x}_E dx_E \end{aligned} \quad \text{Eq. (10)}$$

The vehicle crush energy can be calculated either by using the acceleration of the passenger compartment or by using the barrier force as the crush force. The crush energy calculated from the passenger compartment acceleration (U_A) is as follows:

$$U_A = -(m_P + m_E)\int \ddot{x}dx = -m\int \ddot{x}dx \quad \text{Eq. (11)}$$

Provided that the barrier force F_B is used to calculate the work that made the car deform, the crush energy calculated using the barrier force (U_B) is expressed using Equation 9 as follows:

$$U_B = \int F_B dx = -\int (m_P \ddot{x} + m_E \ddot{x}_E)dx \quad \text{Eq. (12)}$$

Note that U_S, U_A, and U_B are functions of dynamic crush x, while E_A is a function of the residual crush C. From the FE model, the masses are set as m = 1092 kg, m_P = 946 kg, and m_E = 146 kg; and the acceleration of the passenger compartment and the engine was determined in the full frontal impact simulation for an impact velocity V_0 = 55 km/h. The crush energies U_S, U_A, and U_B were compared to the reference value (i.e., the internal energy of the car FE model) in order to examine whether the product of the vehicle mass and the passenger compartment acceleration or the barrier force is more accurate as the crush force to be used in calculating crush energy.

EAF and Impact Velocity In this research, FE simulations of full frontal impact were conducted (see Figure 5(a)). From the full frontal impact simulation, the crush stiffness coefficients d_0 and d_1 of EAF vs. crush were determined for changing impact velocities ranging from 10 to 80 km/h. Designating m as the vehicle mass (1092 kg) and V_0 as the initial velocity, the crush energy E_A is equal to the initial kinetic energy $(1/2)mV_0^2$ in the full frontal impact tests. The relation between EAF ($\sqrt{2E_A/w}$) and the residual crush C_{Ave} was examined from the low to high impact velocities using the FE models. The crush stiffness coefficients d_0 and d_1 in Equation 2 were calculated from this relationship.

In the standard method, the intercept d_0 is determined using the vehicle kinetic energy associated with the speed for the threshold of residual crush. Note that the typical threshold speed is 5 mph. The slope d_1 is calculated such that the line goes through

FIGURE 5 FE simulation conditions. Driver side (left side) was impacted in offset and oblique frontal impact simulations.

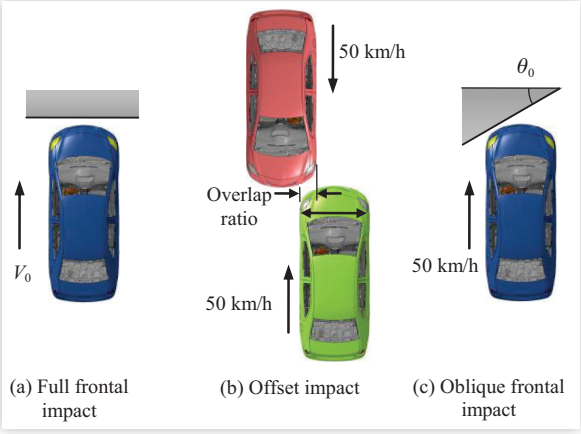

© 2018 SAE International. All Rights Reserved.

This content downloaded from 66.194.72.152 on Thu, 01 Jul 2021 17:05:51 UTC
All use subject to https://about.jstor.org/terms

FIGURE 6 A new method to obtain d_0 and d_1.

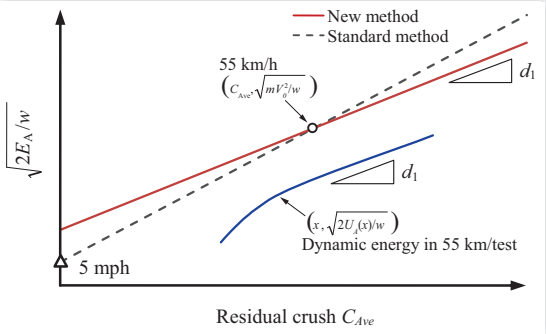

© SAE International

the points of EAF at 5 mph and at the residual crush at the NCAP test speed (i.e., 35 mph or 55 km/h). We examined that the coefficients in Equation 1 can be determined using only the dynamic data in NCAP. In the full frontal impact at 55 km/h in the FE simulation, the crush energy $U_A(x)$ absorbed during the dynamic crush (x) was calculated using Equation 11. Instead of using EAF, the square root of the dynamic crush energy $U_A(x)$ per unit crush width w at dynamic crush (x) was calculated using:

$$\sqrt{\frac{2U_A(x)}{w}} = \sqrt{-\frac{2m\int_0^x \ddot{x}dx}{w}} \qquad \text{Eq. (13)}$$

A new method to obtain the crush stiffness coefficients d_0 and d_1 is proposed (Figure 6) as follows:

1. The slope of the EAF vs. residual crush is determined from the slope of the curve $\sqrt{2U_A(x)}/w$ vs. dynamic crush x.
2. By specifying that the approximation line goes through the point of the residual crush C_{Ave} and EAF ($\sqrt{2E_A/w} = \sqrt{mV_0^2/w}$, V_0 = 15.3 m/s) at 55 km/h, the approximation line of EAF then can be drawn using one crash test at 55 km/h.

This method was applied to the crush energy and dynamic crush in a 55 km/h full frontal impact FE simulation. If the crush stiffness coefficients d_0 and d_1 can be calculated at a velocity of 55 km/h, d_0 and d_1 can be obtained for many car models in NCAP.

Database of Coefficients of EAF Appling the new method to the full frontal impact tests at 55 km/h of JNCAP (2007-2016), the crush stiffness coefficients d_0 and d_1 of various vehicle models were calculated. The dynamic crush versus time can be determined by calculating the double integral of the acceleration of the passenger compartment (B-pillar bottom). The dynamic crush energy with the dynamic crush was computed using Equation 11. It is shown that the vehicle stiffness calculated in the full frontal impact tests tends to be proportional to the vehicle mass [19]. Thus in this study, 1000 kg was adopted as standard car mass, and the EAF coefficients were normalized by this vehicle mass 1000 kg, that is, the EAF was divided by $\sqrt{m/1000}$.

Offset Impact

FE simulations of car-to-car offset frontal impacts with identical car models were conducted at 50 km/h (Figure 5(b)). The driver side (left side) was impacted, and the overlap ratio was changed from 20% to 100% to validate the homogeneous assumption on the vehicle stiffness in a lateral location. The crush energy E_A was calculated from Equation 2 using the crush profile (C_1 to C_6) and the crush stiffness coefficients d_0 and d_1 obtained in the full frontal FE simulation. This crush energy was compared to the reference value (i.e., the sum of internal energy and sliding energy in FE model output). The distribution of internal energy of structures with changing overlap ratios was examined to compare the homogeneous assumption.

Oblique Impact

To validate the correction factor with an angled PDOF in Equation 5, oblique frontal impact simulations were conducted against the rigid barrier at 55 km/h with changing barrier angles θ_0 (Figure 5(c)). The driver side (left side) was impacted. In the oblique impact, the impulse was calculated by calculating the integral of the contact force between the car and the barrier during the time duration of the impact. The angle of PDOF (θ_{PDOF}) was calculated by the impulse in the car in the longitudinal and lateral directions (see Figure 1). The crush energy E_A, calculated using the crush stiffness

© 2018 SAE International. All Rights Reserved.

This content downloaded from
66.194.72.152 on Thu, 01 Jul 2021 17:05:51 UTC
All use subject to https://about.jstor.org/terms

coefficients d_0 and d_1 (determined from a full frontal impact) and the crush profile in the oblique impact (see Equation 2), and its correction energy $E_A(1 + \tan^2 \theta_{PDOF})$ were compared to the reference values (internal and sliding energy of the car FE model). The correction factor by PDOF angle was examined by the barrier angle θ_0 and the angle of PDOF (θ_{PDOF}).

Results

Model Validation

Figures 7 and 8 show the residual crush at the rails and acceleration of the passenger compartment in a full frontal impact at speeds of 55 and 80 km/h, respectively. In the 55 km/h test, the residual crush of the FE model and the tests were comparable. The vehicle acceleration was relatively higher for the FE simulation than for the test. In the 80 km/h test, the tire made contact with the side sill, and the passenger compartment was still intact. The CORA ratings of the acceleration calculated in the FE simulation with respect to that in the tests were 0.70 (55 km/h) and 0.84 (80 km/h). On the basis of ISO rating [16], the acceleration curve in the FE simulation was a fair agreement in the 55 km/h test and was a good agreement in the 80 km/h test. The error of the front rail residual crush in the FE simulation relative to that in the test was 5.7% (right) and 9.7% (left) in the 55 km/h impact, and 4.1% (right) and 0.9% (left) in the 80 km/h impact. From the 55 and 80 km/h tests, the FE model reasonably represents the residual crush and vehicle acceleration in the tests, and therefore it was judged that this model could be used for the analysis in this research.

Crush Force

The accelerations and masses of the passenger compartment and the engine and the barrier force of the car FE model were used to compare the contributions of the forces for the spring-mass model (Figure 4). Figure 9 shows the barrier force, engine force ($-m_E \ddot{x}_E$), and structural force ($-m_p \ddot{x}$) obtained from the car FE model. The trend of the sum of $-m_E \ddot{x}_E$ and $-m_p \ddot{x}$ agrees with that of F_B, which shows that this spring-mass model can be applied for simulating the vehicle impact against the barrier. The high barrier force, occurring at around 0.48 m of vehicle displacement, was caused by the engine dump force against the barrier, whereas this peak was not observed in the acceleration of the passenger compartment.

The crush energies U_S, U_A, and U_B were calculated using the accelerations and the displacements of the small car model in the FE analysis using Equations 10, 11, and 12, and were compared with the reference value (i.e., the vehicle internal energy U obtained from the FE analysis) as shown in Figure 10. The rebound phase was included to calculate these energies (the restitution coefficient e was 0.185 in FE model and 0.182 in the tests at the impact velocity of 55 km/h). U_S agrees with U,

FIGURE 7 Top: Figures of vehicle crush of FE model and test. Bottom: Plots of vehicle acceleration and residual crush (full frontal test at 55 km/h).

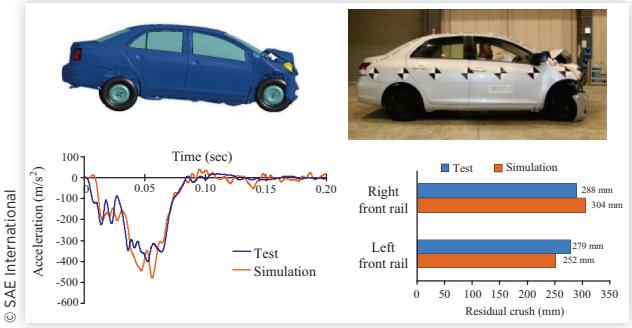

FIGURE 8 Top: Figures of vehicle crush of FE model and test. Bottom: Plots of vehicle acceleration and residual crush (full frontal test at 80 km/h).

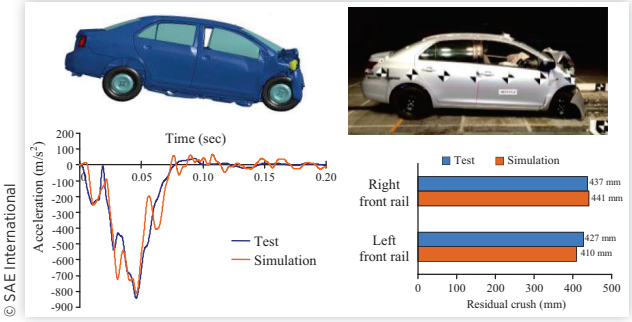

FIGURE 9 The barrier force, structural force, and engine force vs. vehicle displacement obtained from the FE analysis.

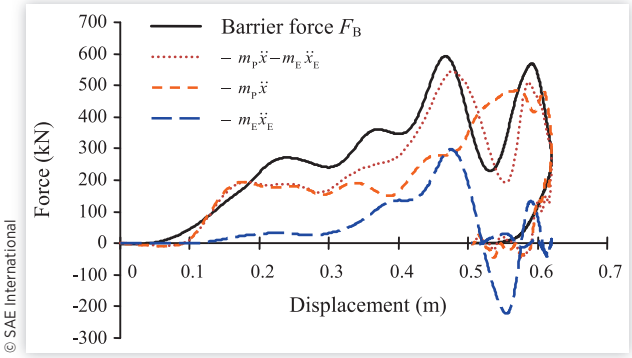

© 2018 SAE International. All Rights Reserved.

This content downloaded from 66.194.72.152 on Thu, 01 Jul 2021 17:05:51 UTC
All use subject to https://about.jstor.org/terms

Case 2:19-cv-01338-JCC Document 80-1 Filed 07/14/21 Page 9 of 15

FIGURE 10 Plot of crush energy calculated from the barrier force and the compartment acceleration compared with the internal energy in the small car FE model.

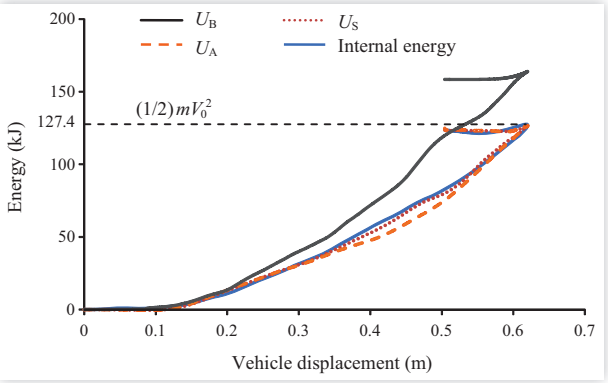

© SAE International

FIGURE 11 EAF and residual crush for various impact velocities in full frontal impact. E_A was calculated by $E_A = (1/2)mV_0^2$.

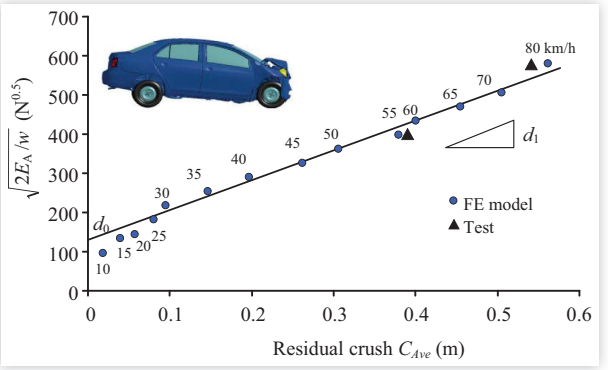

© SAE International

FIGURE 12 The crush energy vs. dynamic crush at 55 km/h compared to EAF vs. residual crush.

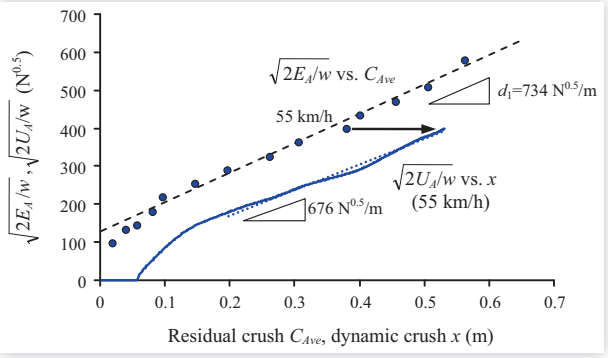

© SAE International

which indicates that the spring-mass model can also be applied for the crush energy calculation including engine dumping. U_A is slightly smaller than U; however, U_B is substantially larger than U ($U_A < U < U_B$). The reason for the large U_B is that the engine acceleration was integrated with respect to the passenger compartment displacement in Equation 12, though the passenger compartment displacement is larger than the engine displacement. The engine deceleration should be integrated with respect to the engine displacement in Equation 10 for an accurate vehicle crush energy. The maximum crush energy of U_A coincides with the initial kinetic energy of the car $\left((1/2)mV_0^2\right)$, and that of U_B is substantially larger than the initial kinetic energy. The crush energy is likely overestimated when the barrier force is used as the crush force since the engine dump force has a large effect on the barrier force.

EAF and Impact Velocity Simulations of the full frontal impact tests at impact velocities ranging from 10 to 80 km/h were conducted using the car FE model. Figure 11 shows EAF vs. the average residual crush C_{Ave}. It is observed that the EAF has a linear relation with residual crush in the speed range from 30 to 80 km/h. By applying the least squares method for this velocity range, the crush stiffness coefficients d_0 and d_1 are 139 N$^{0.5}$ and 734 N$^{0.5}$/m, respectively. For impact velocities of 25 km/h or less, EAF was lower than the approximation line.

In Figure 12, the curve of $\sqrt{2U_A(x)/w}$ vs. dynamic crush (x) is plotted along with the curve of EAF vs. residual crush C_{Ave}. The maximum crush energy at 55 km/h coincides with $\sqrt{2U_A(x_{max})/w}$ and EAF. Because the dynamic car crush is larger than the residual car crush, the curve of $\sqrt{2U_A(x)/w}$ vs. dynamic crush shifts to the right of the curve of EAF vs. residual crush. The mean slope of $\sqrt{2U_A(x)/w}$ vs. dynamic crush (x) was 676 N$^{0.5}$/m for a dynamic crush of 0.2 m or more. This crush of 0.2 m was chosen because the left and right fenders started to contact the barrier at the dynamic crush of 0.2 m. This slope approximates the d_1 (734 N$^{0.5}$/m) with an error of 7.9%. This is likely due to the incremental dynamic crush being close to the incremental residual crush in the range of high-velocity impacts where the restitution coefficient e is small. The restitution coefficient decreases with increasing impact velocity, and it varies from 0.2 to 0.1 in impact velocities in the range from 30 to 55 km/h [20]. Therefore, it was observed that the slope of $\sqrt{2U_A(x)/w}$ agreed with d_1 for the velocity range where the restitution coefficient is stable.

Figure 13 shows the coefficients of EAF determined from this new method and from the standard method (d_0 correspond to the kinetic energy at 5 mph). Both approximation lines go through the point of EAF and the residual crush at 55 km/h. In Figure 13, the EAF determined from the new method is closer to the actual EAF than that determined from the standard method using the residual crush in the range 0.1 to 0.4 m.

Database of Coefficients of EAF Figure 14 shows curves of EAF vs. residual crush for various vehicle models classified by minicar, car with transverse engine, car with longitudinal engine, minivan, and sport-utility vehicle (SUV). Table 1 presents the average value of d_0 and d_1 among the vehicle classes.

© 2018 SAE International. All Rights Reserved.

This content downloaded from
66.194.72.152 on Thu, 01 Jul 2021 17:05:51 UTC
All use subject to https://about.jstor.org/terms

Minicars have a large value of d_1, which indicates that minicars have a higher stiffness. Other vehicle types have comparable values of d_1 when normalized with vehicle mass.

Offset Impact

Offset frontal car-to-car test simulations were carried out using various overlap ratios. The crush energy E_A, calculated from Equation 2 based on the crush profile and the crush stiffness coefficients (d_0 139 $N^{0.5}$, d_1 734 $N^{0.5}$/m), was compared to the sum of the internal energy and sliding energy (reference value) as shown in Figure 15. The crush energy agrees with the sum of internal energy and sliding energy in the FE model output for an overlap ratio ranging from 40% to 100%, where at least one front rail was involved (note that the front rail was partly involved in the 40% overlap). In the overlap ratios of 20% and 30%, the sum of the internal and sliding energy was small since the car did not stop due to the car's translational and rotational motion resulting from its kinetic energy. In these small overlap collisions, the crush energy calculated from the crush profile is smaller than the sum of internal energy and sliding energy. This is because the crush depth was limited by the side sill as well as the firewall. In addition, the crush width was narrow and the induced damage was not wider because the direct damage was outside of the front rail.

Figure 16 shows the internal energy of each structure of the FE model output. In a 100% overlap, the crush boxes and front rails accounted for 54.8% of total internal energy. As the overlap ratio decreased until it reached 50%, the internal energy of the crush box and front rail of the impact side (i.e., the left side) remained the same, whereas those of the non-impacted side decreased consistently. Although the energy distributions of each component changed with the overlap ratio, the internal energy did not change substantially when at least one front rail was involved.

Oblique Impact

In the oblique impact at 55 km/h, the crush energy was calculated based on the crush profile with the crush stiffness coefficients (d_0 = 139 $N^{0.5}$, d_1 = 734 $N^{0.5}$/m), and was compared to the internal energy calculated by the FE model. Figure 17 shows the FE internal energy E_A, the crush energy calculated by crush depth measured along car longitudinal direction (Equation 2), and the crush energy multiplied by the correction factor $E_A(1 + \tan^2 \theta_{PDOF})$. As the barrier angle θ_0 increased, the FE internal energy decreased consistently. Moreover, the energy loss caused by the car sliding against the barrier increased. When comparing the sum of the internal energy and the sliding energy as a reference value, the crush energy calculated by crush profile E_A is relatively comparable for impact angles ranging from 0 to 30 degrees: the errors range from 3.1% to 13.6% for E_A and 2.4% to 13.8% for $E_A(1 + \tan^2 \theta_{PDOF})$ with respect to the reference value (sum of internal energy and sliding energy). In the range from 35 to 45 degrees, E_A and $E_A(1 + \tan^2 \theta_{PDOF})$ were smaller than the sum of the internal energy and the sliding energy: the errors range from 14.9% to 61.6% for E_A and 4.9% to 50.2% for $E_A(1 + \tan^2 \theta_{PDOF})$. When the PDOF is 35 degrees or more, the $E_A(1 + \tan^2 \theta_{PDOF})$ is closer to the sum of the internal energy and the sliding energy than E_A.

FIGURE 13 A procedure to draw the EAF approximation line.

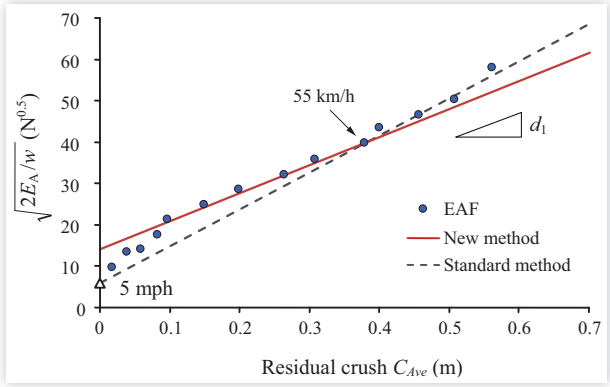

© SAE International

FIGURE 14 EAF vs. residual crush for various types of vehicles in JNCAP (2007-2016).

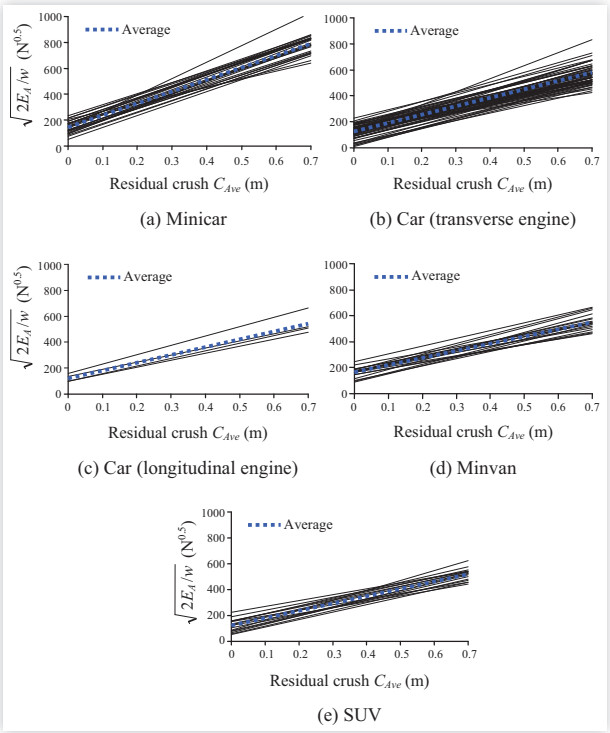

© SAE International

© 2018 SAE International. All Rights Reserved.

This content downloaded from
66.194.72.152 on Thu, 01 Jul 2021 17:05:51 UTC
All use subject to https://about.jstor.org/terms

TABLE 1 The crush stiffness coefficients d_0 and d_1 in JNCAP.

	$\sqrt{2E_A/W} = d_0 + d_1C$				
		Average		Standard deviation	
Vehicle type	n	d_0 ($N^{0.5}$)	d_1 ($N^{0.5}$/m)	d_0 ($N^{0.5}$)	d_1 ($N^{0.5}$/m)
Minicar	26	146.2	917.0	46.7	111.2
Car (transverse engine)	58	124.7	626.2	49.9	103.0
Car (longitudinal engine)	4	122.4	600.7	27.2	71.9
Minivan	18	161.4	558.4	40.4	86.3
SUV	16	121.6	566.0	47.9	80.4

The coefficient is scaled for a vehicle mass of 1000 kg. The $\sqrt{m/1000}$ should be multiplied for d_0 and d_1 with vehicle mass of m (kg).

© SAE International

Figure 18 shows the ratio of E_A to the sum of internal energy and sliding energy, and the factor $(1 + \tan^2 \theta_{PDOF})$. The ratio of E_A to the sum of internal energy and sliding energy is distributed around 1.0 for the PDOF for impact angles ranging from 0 to 30 degrees, and it is larger than the factor $(1 + \tan^2 \theta_{PDOF})$ for the PDOF for impact angles of 35 degrees or more.

FIGURE 15 The crush energy in car-to-car offset impact with changing overlap ratio: maximum sum of internal energy and sliding energy from FE model output, energy calculated by crush profile.

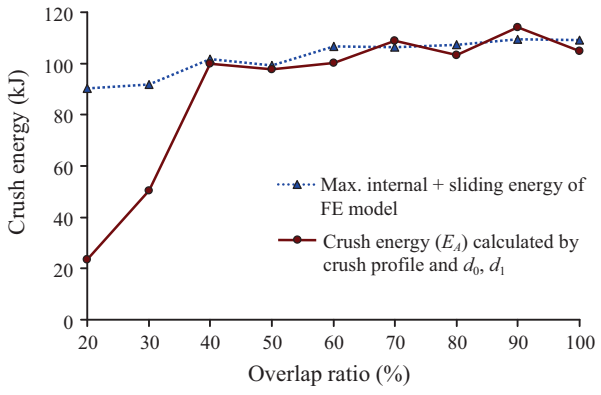

© SAE International

FIGURE 16 The internal energy of each structure with overlap ratio in offset car-to-car crash in the FE simulation.

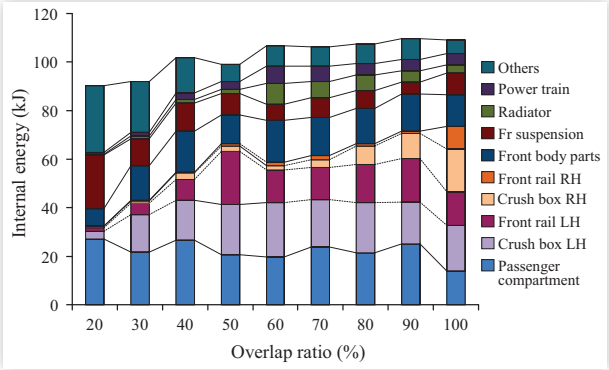

© SAE International

Discussion

Tavakoli et al. [21] conducted FE simulations in which a car underrides against a truck's frontal structure. They showed that FE analysis is a useful tool to obtain the relationship between the crush energy and the crush profile with a complicated shape involved in the underride. In this research study, a series of FE analyses of a small car were conducted to validate the theory of crush energy used in accident reconstructions, which were established based on various crash tests. The internal energy calculated from using the FE model is available as a reliable reference value, and can be compared to the crush energy calculated using the crush profile in the accident reconstruction. Furthermore, the internal energy and the kinetic energy of each structure from the FE analysis provide useful information to validate the theories currently used in accident reconstructions.

The force-crush characteristics are the basis from which to determine the vehicle crush energy. The barrier force or the vehicle acceleration in full frontal impact test may be utilized to represent the crash force. In full frontal tests, the engine dump force leads to a high barrier force. In this research, it was shown that the crush energy calculated using the barrier force was larger than that from using the FE internal energy and the energy of the spring-mass model. This was caused by the high barrier force of the engine dump, which is observed to occur in full frontal rigid barrier tests [17, 18]. Hence, it is recommended that the passenger compartment acceleration be used to calculate the vehicle crush energy.

The linear relation between the EAF and crush is the basis of energy-based accident reconstructions. In the FE analyses conducted for this research, the EAF had a linear relationship with the average residual crush. In previous research using vehicles before the 2000 model year, the slope of the EAF vs. residual crush curve decreased with the average residual crush

© 2018 SAE International. All Rights Reserved.

This content downloaded from 66.194.72.152 on Thu, 01 Jul 2021 17:05:51 UTC
All use subject to https://about.jstor.org/terms

for impact speeds above the 30 mph or 35 mph test because of the passenger compartment collapsing at the higher impact velocities [6, 8]. In contrast, Bare et al. [22] conducted a series of tests, including high-speed impact tests at 50 mph (80 km/h), and found that vehicle stiffness can be approximated using linear constant characteristics. In this research, a full frontal test of a small car at 80 km/h was conducted, and the passenger compartment did not collapse but instead experienced limited passenger compartment intrusion. This small car was designed to satisfy the criteria for the offset deformable barrier (ODB) test at 64 km/h in NCAP test. In the ODB tests in the current NCAP, the passenger compartment remains intact and experiences small intrusion. Thus, it is likely that the linear approximation can be used for the EAF vs. residual crush curve for vehicles that ODB tests were carried out at 64 km/h in NCAP. It is not clear whether the linear approximation can be applied for a velocity higher than 80 km/h; however, the linear relation can be used for a practical impact velocity. In addition to the collapse of the passenger compartment, the effect of the vehicle pitching behavior during a crash needs to be included at such a high impact velocity.

A new method to determine the crush stiffness coefficients d_0 and d_1 in full frontal tests was proposed. In general, to calculate the crush stiffness coefficients d_0 and d_1, results from crash tests at 55 km/h and the 5 mph intercept are used, though this method was proposed in 1990 [5]. The bumper material and crush boxes have changed since then. In this research, a new method was proposed, which uses only the data of full frontal impact test at 55 km/h. As a follow-up step, it is necessary to validate whether this method has a higher precision for approximating EAF than that using the standard method with the 5 mph intercept. Furthermore, real-world collisions occur frequently in this velocity range.

The assumption of homogeneous stiffness was verified in the car-to-car offset frontal crashes with an overlap ratio from 40% to 100% where at least one front rail is involved. However, this assumption cannot be applied for small overlap collisions where the front rails are not involved. In small overlap impacts, different EAF coefficients need to be determined. It is probable that the small overlap impact tests conducted by the Insurance Institute for Highway Safety can be employed to determine the crush characteristics where the front rails are not involved. As shown in Figure 16, the distributions in internal energy of each structure change with overlap ratio, whereas the sum of internal energy and sliding energy remains constant for an overlap ratio ranging from 60% to 100%. This is because once the crash configuration is known, the energy loss can be calculated in planar impact mechanics, which are independent of vehicle stiffness.

In oblique impacts, the correction factor $(1 + \tan^2 \theta_{PDOF})$ for crush energy has a large value, that is, the factor is 2.0 for an impact angle of 45 degrees. In this study, the crush energy calculated E_A without using the correction factor for the angle is close to the sum of internal and sliding energy determined from the FE model simulations for angles less than 30 degrees of barrier angle (errors distributed from 3.1% to 13.6%). Monk et al. [23] showed that the ratio of crush energy calculated with crush profile to the crush energy calculated by kinetic energy remained almost constant with barrier angles from 0 to 55 degrees. In oblique impact FE simulation, as the angle increased, the energy loss resulting from the sliding between the car and barrier was larger (Figure 17). Moreover, the front

FIGURE 17 The crush energy in oblique impact: maximum internal energy of FE model, energy calculated by crush profile, and the crush energy with correction factor. E_A was calculated by d_0, d_1, and crush depth measured along the car longitudinal direction.

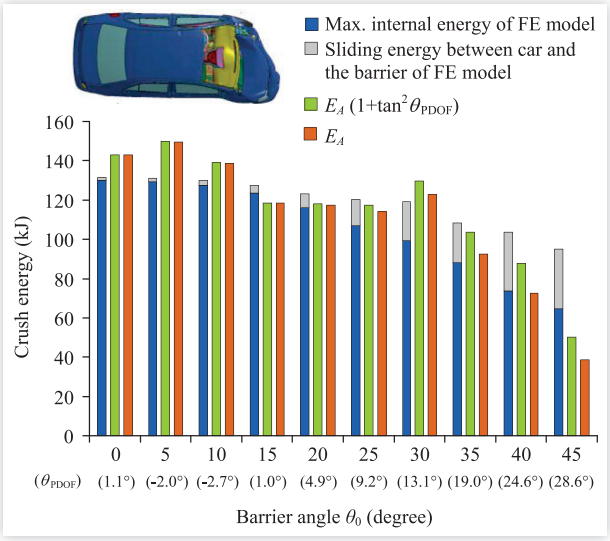

© SAE International

FIGURE 18 The ratio of the sum of internal energy and sliding energy to E_A, and the crush energy correction factor in oblique impact.

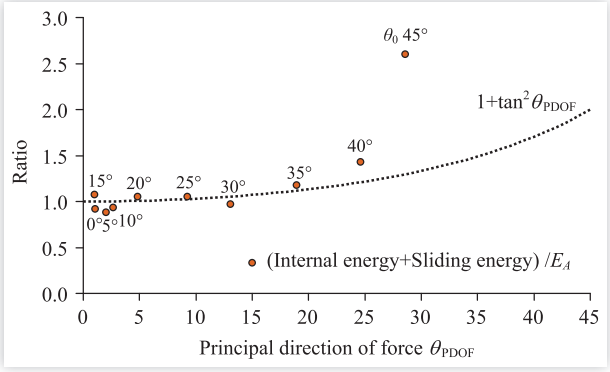

© SAE International

© 2018 SAE International. All Rights Reserved.

This content downloaded from
66.194.72.152 on Thu, 01 Jul 2021 17:05:51 UTC
All use subject to https://about.jstor.org/terms

rails did not collapse in their axial directions, but instead bent laterally, which led to a lower crush energy. Even though the ratio of the crush energy (including the sliding energy) in oblique impacts to the crush energy calculated by the car longitudinal crush profile increased with PDOF angles of 20 degrees or more (see Figure 18), this outcome was not reproduced using the theory of Equations 4 and 5, but was captured by including the sliding energy loss. Hence, the vehicle structure is not isotropic, and it is recommended that the crush energy be calculated without the correction factor of PDOF less than 20 degrees. Brach et al. [9] indicate that the delta-V can be calculated in planar impact mechanics without input of PDOF. Hence, for the PDOF angles of 20 degrees or more, planar impact mechanics will be appropriate to calculate the delta-V.

Conclusions

In this research, the method to calculate the crush energy in accident reconstruction was investigated using an FE model of a small car.

1. In calculating the crush energy, the barrier force can overestimate the crush energy if it is used as the crush force because of the engine dump. When the product of vehicle mass and vehicle acceleration was used as the crush force, the crush energy was close to the actual crush energy as determined by the FE model.
2. In the full frontal impact simulations, the EAF has a linear relationship with the residual crush in the impact velocity range from 30 to 80 km/h. The slope of the curve of the square root of crush energy per vehicle crush width vs. dynamic crush agreed with that of the curve for EAF vs. residual crush. Thus, the approximation line of EAF can be drawn using this slope by having it pass through the point of the EAF and the residual crush of the 55 km/h full frontal test.
3. From the car-to-car offset frontal impact simulations, it was confirmed that the homogeneous behavior assumption across the crush width is valid where at least one front rail is involved. In small overlap collisions, the energy calculated from the crush profile with EAF coefficients is less than the car internal energy.
4. In oblique impacts against the barrier with large angles, the initial kinetic energy was lost as a result of the sliding between the car and barrier. In oblique frontal impacts with PDOF angles ranging from 0 to 20 degrees, the crush energy calculated without using the correction factor associated with the angle is close to the sum of the car internal energy and sliding energy.

Acknowledgment

This research was conducted in the project of “Development of technology for accident database” under the budget of the Ministry of Economy, Trade, and Industry, Japan.

References

1. Emori, R., “Analytical Approach to Automobile Collisions,” SAE Technical Paper 680016, 1968, doi:10.4271/680016.
2. Campbell, K., “Energy Basis for Collision Severity,” SAE Technical Paper 740565, 1974, doi:10.4271/740565.
3. McHenry, R., “User’s Manual for the Crash Computer Program,” Calspan Report No. ZQ-5708-V-3, Contract No. DOT-HS-5-01124, 1976.
4. Prasad, A., “CRASH3 Damage Algorithm Reformulation for Front and Rear Collisions,” SAE Technical Paper 900098, 1990, doi:10.4271/900098.

© 2018 SAE International. All Rights Reserved.

This content downloaded from
66.194.72.152 on Thu, 01 Jul 2021 17:05:51 UTC
All use subject to https://about.jstor.org/terms

5. Strother, C., Woolley, R., and James, M., "A Comparison between NHTSA Crash Test Data and CRASH3 Frontal Stiffness Coefficients," SAE Technical Paper 900101, 1990, doi:10.4271/900101.
6. Struble, D.E., *Automotive Accident Reconstruction: Practices and Principles* (Boca Raton, FL: CRC Press, 2013).
7. Kerkhoff, J., Husher, S., Varat, M., Busenga, A. et al., "An Investigation into Vehicle Frontal Impact Stiffness, BEV and Repeated Testing for Reconstruction," SAE Technical Paper 930899, 1993, doi:10.4271/930899.
8. Varat, M., Husher, S., and Kerkhoff, J., "An Analysis of Trends of Vehicle Frontal Impact Stiffness," SAE Technical Paper 940914, 1994, doi:10.4271/940914.
9. Brach, R.M. and Brach, R.M., "Crush Energy and Planar Impact Mechanics for Accident Reconstruction," SAE Technical Paper 980025, 1998, doi:10.4271/980025.
10. Fonda, A., "Crush Energy Formulations and Single-Event Reconstruction," SAE Technical Paper 900099, 1990, doi:10.4271/900099.
11. Woolley, R., "Non-Linear Damage Analysis in Accident Reconstruction," SAE Technical Paper 2001-01-0504, 2001, doi:10.4271/2001-01-0504.
12. Hunter, R., Fix, R., Lee, F., and King, D., "Using Force-Displacement Data to Predict the EBS of Car into Barrier Impacts," SAE Technical Paper 2016-01-1483, 2016, doi:10.4271/2016-01-1483.
13. Oga, R., Ide, Y., and Ikari, T., "Construction of Energy Absorption Diagram Based on Experimental Data in Japanese New Car Assessment Program," *Review of Automotive Engineering* 29:111-113, 2008.
14. Gabler, H.C., Hinch, J.A., and Steiner, J., *Event Data Recorders: A Decade of Innovation* (SAE International, 2008).
15. Marzougui, D., Samaha, R., Cui, C., and Kan, C., "Extended Validation of the Finite Element Model for the 2010 Toyota Yaris Passenger Sedan," Working Paper, NCAC 2012-W-005, 2012.
16. International Organization for Standardization (ISO), "Road Vehicles - Objective Rating Metric for Non-Ambiguous Signals," ISO/TS 18571, 2014.
17. Johanssen, H., Adolph, T., Thomson, R., Edwards, M. et al., "FIMCAR - Frontal Impact and Compatibility Assessment Research: Strategy and First Results for Future Frontal Impact Assessment," *22nd ESV*, Washington, DC, June 13-16, 2011.
18. Yonezawa, H., Mizuno, K., Hirasawa, T. et al., "Summary of Activities of the Compatibility Working Group in Japan," *21st ESV*, Stuttgart, Germany, June 15-18, 2009.
19. Mizuno, K., *Crash Safety of Passenger Vehicles* (Nagoya University Press, 2012) (in Japanese).
20. Wood, D., "Structural Rebound Characteristics of the Car Population in Frontal Impacts," SAE Technical Paper 2000-01-0461, 2000, doi:10.4271/2000-01-0461.
21. Tavakoli, M., Valliappan, P., Pranesh, A., and Savage, C., "Estimation of Frontal Crush Stiffness Coefficients for Car-to-Heavy Truck Underride Collisions," SAE Technical Paper 2007-01-0731, 2007, doi:10.4271/2007-01-0731.
22. Bare, C., Peterson, D., Marine, M., and Welsh, K., "Energy Dissipation in High Speed Frontal Collisions," SAE Technical Paper 2013-01-0770, 2013, doi:10.4271/2013-01-0770.
23. Monk, M. and Guenther, D., "Update of Crash2 Computer Model Damage Tables," VRTC-SRL-16, DOT HS-806 446, 1983.

© 2018 SAE International. All rights reserved. No part of this publication may be reproduced, stored in a retrieval system, or transmitted, in any form or by any means, electronic, mechanical, photocopying, recording, or otherwise, without the prior written permission of SAE International.

Positions and opinions advanced in this work are those of the author(s) and not necessarily those of SAE International. Responsibility for the content of the work lies solely with the author(s).

This content downloaded from
66.194.72.152 on Thu, 01 Jul 2021 17:05:51 UTC
All use subject to https://about.jstor.org/terms

This content downloaded from
66.194.72.152 on Thu, 01 Jul 2021 17:05:51 UTC
All use subject to https://about.jstor.org/terms